

ENVIRONMENTAL RESEARCH
LETTERS

LETTER

OPEN ACCESS

RECEIVED
11 October 2024REVISED
7 February 2025ACCEPTED FOR PUBLICATION
13 February 2025PUBLISHED
28 February 2025

Original content from
this work may be used
under the terms of the
[Creative Commons
Attribution 4.0 licence](#).

Any further distribution
of this work must
maintain attribution to
the author(s) and the title
of the work, journal
citation and DOI.

Assessment of global land cover changes using satellite data:
intermittent and long-term land cover changes from 2001 to 2020Shuo Chen¹ , Qianlai Zhuang^{1,2,*} , Farzad Taheripour³ , Ye Yuan¹ and Lauren Benavidez³ ¹ Department of Earth, Atmospheric, Planetary Sciences, Purdue University, West Lafayette, IN 47907, United States of America² Department of Agronomy, Purdue University, West Lafayette, IN 47907, United States of America³ Department of Agricultural Economics, Purdue University, West Lafayette, IN 47907, United States of America

* Author to whom any correspondence should be addressed.

E-mail: qzhuang@purdue.edu**Keywords:** land cover change, cropland expansion, forest decline, uncertainty in satellite dataSupplementary material for this article is available [online](#)

Abstract

Global land cover has changed during the past decades, influencing biogeochemical cycles and the global climate system. This study aimed to improve understanding of global land cover dynamics to enable more effective future land management practices and conservation actions. This study quantified interannual changes in global land cover types from 2001 to 2020 and distinguished intermittent transitions from stable gains and losses. From the interannual perspective, we found that global barren lands, forests, shrublands, and snow-covered areas decreased by 5281, 1804, 952, and 188 kha yr⁻¹, respectively. In contrast, grasslands, croplands, urban areas, and water bodies increased at 6529, 1407, 237, and 51 kha yr⁻¹, respectively, from 2001 to 2020. According to the definitions provided in this paper, of the global forest areas, 75% was Stable (no change), 4% was Gain, 5% was Loss, and 16% was Unstable. Of the cropland areas, 56% was Stable, 9% was Gain, 9% was Loss, and 26% was Unstable. Hotspots for forest loss were Brazil, the Rest of South America, and Sub-Saharan Africa, and grassland was the most common land cover classification following forest loss. The global cropland expansion hotspots were Brazil, Canada, China, India, and the Rest of South America. The cropland gains were mainly converted from grasslands. On the other hand, barren areas in China and Middle Eastern and North Africa were changed to grasslands. A certain amount of shrublands were changed to forest in temperate regions. This paper provided land cover changes at a 500 m spatial resolution as a benchmark for future assessments. The findings showed that unstable pixels play an important role in determining the sources of uncertainty when assessing land cover changes using satellite data. Land cover assessments are sensitive to the time steps used for analysis and the definition of changes.

1. Introduction

Global land covers have changed over time, and their patterns and causes vary by region (Luyssaert *et al* 2014, Shukla *et al* 2019, Winkler *et al* 2021). Particularly, over the past two decades, deforestation has continued to occur across the world with different drivers and incentives. These include initial incursions into forests for extractive enterprises and agricultural activities, infrastructure expansion, development programs, and land-grabbing incentives in areas with weak property rights (Laurance *et al* 2009, Barber *et al* 2014, Engert *et al* 2024). Cropland

has declined in some countries due to urbanization (Liu *et al* 2019, Qiu *et al* 2020). Overgrazing and logging have accelerated desertification in arid and semi-arid regions (Song *et al* 2018). Meanwhile, temperate zones have experienced forest expansion driven by afforestation activities (Bryan *et al* 2018, Piao *et al* 2020).

A better understanding of how global land cover changes across time and space is important to enable the design of effective climate adaptation and mitigation measures. Prior research underscored the need for detailed analysis of land cover change over time to understand when, where, and how land covers have

changed (Efroymson *et al* 2013). This study improved documentation and understanding of global land cover dynamics to enable more effective future conservation actions and policies. The land cover statistics by country from the Food and Agriculture Organization of the United Nations (FAOSTAT) are useful for quantifying land cover change at a macro scale by country. However, they cannot meet the demand for finely detecting and quantifying the change in land cover across time and space due to their coarse spatial resolutions (Goldewijk *et al* 2017, Liu *et al* 2018). This study filled this research gap by analyzing land cover changes at the gridded level.

The existing gridded land cover change studies rarely distinguished between the long-term and intermittent changes in land covers (Song *et al* 2018, Liu *et al* 2020, Jing *et al* 2024). However, distinguishing these two types of changes is important to evaluate the impact of land cover changes. For example, in areas where forestry is the primary industry, fallen trees are typically processed into the supply chain for wood and fiber, and the deforested areas will often recover within a few years. Therefore, these areas should not be regarded as permanent deforestation when assessing the success of the zero-deforestation commitment (Curtis *et al* 2018). Similarly, when we evaluate the changes in soil organic carbon (SOC) of cropland, it is crucial to separate the long-term (e.g. cropland expansion) and intermittent changes (e.g. cultivation-fallow rotation). This study classified the observed land cover changes between 2001 and 2020 into long-term and intermittent categories, as defined in section 2.4. We then analyzed these changes at a global scale at a 500 m resolution to address the following questions:

- (1) Which land cover types and regions have undergone the greatest changes from 2001 to 2020?
- (2) What were the sources of gains and losses in alternative land types between 2001 and 2020 by grid cells across the globe?

This information is useful to inform future research and initiatives to mitigate the changes that are most detrimental to conservation, climate and development goals.

The existing literature has addressed uncertainties in assessing land cover changes using gridded satellite data sets (Singh *et al* 2017, Copenhagen 2022, Copenhagen and Mueller 2024). As outlined in the next section of this paper, we mainly analyzed land cover changes using one of the trustable satellite data sets that have been frequently used to study land cover changes: MODIS Collection 6.1 (Sulla-Menashe *et al* 2019). However, to address uncertainties in land cover assessments, we evaluated land cover changes using another satellite data set, ESA-CCI (Defourny *et al* 2017), that also represents land cover changes over

time. The results obtained from the MODIS data set were presented in the main manuscript, while the results obtained from the ESA-CCI were partially shown in the supporting materials.

2. Data and method

2.1. Source of data

The spatial and temporal dynamics of the different land cover classes were derived from the MODIS Collection 6.1 Global Land Cover Classification Systems (LCCS) Land Cover Types product (MCD12Q1) at a 500 m spatial resolution for the period 2001–2020 (Sulla-Menashe *et al* 2019). MCD12Q1 provides global land cover classifications at yearly intervals, relying on consistent satellite data sources (MODIS Aqua and Terra satellites). This product has been widely used to parameterize land surface properties in climate and ecosystem models (Sulla-Menashe *et al* 2019). It also serves as an important input for multiple MODIS land data (e.g. NPP) and facilitates seamless data integration for studying land cover changes and their environmental impacts. Compared with its previous version (MCD12Q1 Collection 5), the year-to-year comparability of MCD12Q1 Collection 6.1 has been significantly improved by using the hidden Markov model algorithm. Specifically, the proportion of land pixels that experienced label changes each year has dropped from 11.4% (Collection 5) to 1.6% (Collection 6) (Sulla-Menashe *et al* 2019). Here, we used ‘LC_Prop2’ land cover layers of MCD12Q1 (Friedl and Sulla-Menashe 2022) in accordance with the FAOSTAT Land Cover Methodology Note (Fao 2024).

We also used the European Space Agency (ESA) Climate Change Initiative (CCI) land cover data (Defourny *et al* 2017) to highlight the fact that different satellites will provide different estimates of historical global land cover changes. This addressed uncertainties in analyzing land cover changes using satellite data.

2.2. Land cover types and aggregations

The MODIS and ESA data sources represent 11 and 22 land cover classes, respectively, as presented in tables S1 and S2. We converted MODIS and ESA-CCI land cover classes into the land cover types defined by the FAOSTAT Land Cover Methodology Note (Fao 2024). Table 1 describes the mapping of MODIS data to FAOSTAT classifications, and table S3 describes the mapping of ESA-CCI data to FAOSTAT classifications.

To analyze data at the country level, we mapped the gridded data to a county level using the World Countries Generalized boundary (URL: <https://hub.arcgis.com/datasets/esri:world-countries-generalized/>). The results of this research could be used to revise the land cover data embedded in

Table 1. Mapping of MCD12Q1 land cover classes to FAOSTAT classification.

Acronym	FAOSTAT classification	FAOSTAT regional area aggregation
Forest	Tree-covered areas	class10 + class20 + 0.40 * class25
Grassland	Grasslands	class30 + 0.20 * class35
Shrubland	Shrub-covered areas	class40 + 0.20 * class35
Cropland	Herbaceous crops	class36 + 0.60 * (class25 + class35)
Barren	Terrestrial barren land	class1
Water	Inland water bodies	class3
Ice	Permanent snow and glaciers	class2
Urban	Artificial surfaces	class9

the GTAP-BIO database, which has been frequently used in analyzing global land cover change studies (Taheripour *et al* 2019, Zhao *et al* 2021, Busch *et al* 2022). Therefore, we further aggregated the country-level data to the 19 regions classified in this model, as presented in table 2 and figure S11.

2.3. Interannual land cover changes

We quantified the annual average area differences for all land cover types presented in table 1 from 2001 to 2020. First, the annual land cover area of the 19 geographical regions presented in table 2 was aggregated from the gridded-level land cover data. For example, the cropland area of a region r is calculated as the sum of area values of class 36 plus 60% of the area from the mosaic classes 25 and 35, respectively. Then, the annual average area difference of land cover type was calculated as:

$$\bar{A}_{ir} = \frac{\sum_{t=2001}^{2020} (A_{irt} - A_{ir(t-1)})}{19},$$

where \bar{A}_{ir} , r , t , and i refer to annual average area difference, region, year, and land cover type, respectively.

2.4. Definition of long-term and intermittent land cover change categories

The observed changes in the area of each grid cell have been classified into four groups: Stable, Unstable, Loss, and Gain, as defined in table 3. For a given land cover type (L_i) in 2001: (1) Stable refers to the pixels that represent no change in their land cover type between 2001 and 2020; (2) Gain refers to the pixels that were not classified as L_i in 2001 and then changed to L_i and remained in the new land cover type for the rest of the years; (3) Loss refers to the pixels that were classified as L_i in 2001 but changed to L_j ($i \neq j$) and never changed to the original or other land cover types in the rest of the years. Changes in land cover for a period of fewer than 5 years were not considered as Gain or Loss; and (4) Unstable refers

to the pixels that represent other types of changes in their land cover type between 2001 and 2020.

3. Results

3.1. Global land cover changes from 2001 to 2020

This section examines average annual changes (including all types of changes) by land cover type and region. Globally, barren lands, forests, shrublands, and snow-covered areas decreased, while grasslands, croplands, urban areas, and inland water bodies increased from 2001 to 2020 (table 4). The barren area has been decreasing in all regions globally, with an average of $-5281 \text{ kha yr}^{-1}$ over the past two decades. China, East Europe and the Rest of Former Soviet Union, and Middle Eastern and North Africa had the largest barren land decreases. In forest areas, Brazil ($-1373 \text{ kha yr}^{-1}$), Sub-Saharan Africa ($-1073 \text{ kha yr}^{-1}$), and the Rest of South America ($-1008 \text{ kha yr}^{-1}$) experienced the greatest reductions. However, the forest area was found to increase the most in China (619 kha yr^{-1}) and Russia (513 kha yr^{-1}). The shrubland area declined across most regions, with the largest decline occurring in Sub-Saharan Africa ($-1062 \text{ kha yr}^{-1}$). On the other hand, shrubland increased in Oceania by 1434 kha yr^{-1} . Global permanent snow and glaciers (Ice) decreased by an average of -188 kha yr^{-1} . Canada and the USA showed noteworthy permanent snow and glacier area decreases of -146 kha yr^{-1} and -125 kha yr^{-1} , respectively.

Grassland area increased in most regions, except for Oceania and India. Sub-Saharan Africa experienced the largest annual grassland area increases by 3652 kha yr^{-1} , while Oceania and India experienced the largest grassland reductions of $-1299 \text{ kha yr}^{-1}$ and -932 kha yr^{-1} , respectively. Global cropland area increased by 1407 kha yr^{-1} . India (882 kha yr^{-1}) and Brazil (651 kha yr^{-1}) had the largest cropland increases. Sub-Saharan Africa had the largest cropland reduction by $-1192 \text{ kha yr}^{-1}$. Urban area increased in all regions, with a global increase of 237 kha yr^{-1} , of which China accounted for more than half of the expansion (121 kha yr^{-1}). Compared with other land cover types, the net change in global inland water bodies was smaller, with an average increase of 51 kha yr^{-1} . Oceania had the largest inland water bodies decrease with an average of -27 kha yr^{-1} .

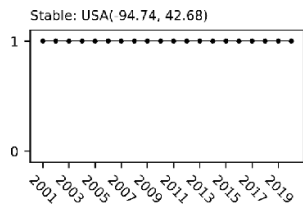
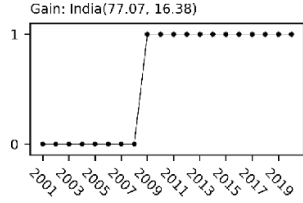
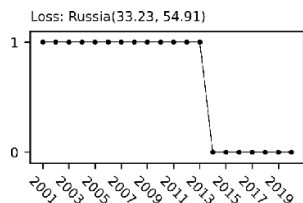
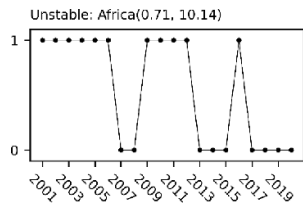
Figure 1 shows the positive and negative extreme annual changes in forest, grassland, shrubland, cropland, and barren land. In forest areas, China experienced positive changes in most years (figure 1(a)). Brazil experienced major negative changes in 2003 and 2015–2017 (figure 1(f)), which to some extent might be partially attributed to wildfires documented in those years (Tyukavina *et al* 2022). In grassland areas, Sub-Saharan Africa experienced major positive changes in 2002–2006 (figure 1(b)).

Table 2. GTAP-BIO 19 regions and their area.

Acronym	Full Name ^a	Total area (kha)
USA	United States	944 506
EU27	European Union 27	634 684
Brazil	Brazil	850 381
Canada	Canada	989 764
Japan	Japan	37 039
ChiHkg	Mainland China and Hong Kong	938 877
India	India	315 822
C_C_Amer	Central and Caribbean Americas	270 042
S_O_Amer	Rest of South America (excluding Brazil)	917 265
E_Asia	East Asia	177 792
R_SE_Asia	Rest of South East Asia	223 456
Mala_Indo	Malaysia and Indonesia	220 869
R_S_Asia	Rest of South Asia	190 894
Russia	Russia	1690 887
Oth_CEE_CIS	East Europe and the Rest of Former Soviet Union	631 407
Oth_Europe	Rest of European Countries	46 214
MEAS_NAfr	Middle Eastern and North Africa	1098 714
S_S_Afr	Sub Saharan Africa	2419 970
Oceania	Oceania	851 388

^a Figure S11 represents members of each region presented in this table.

Table 3. Definition of stable, gain, loss, and unstable land cover.

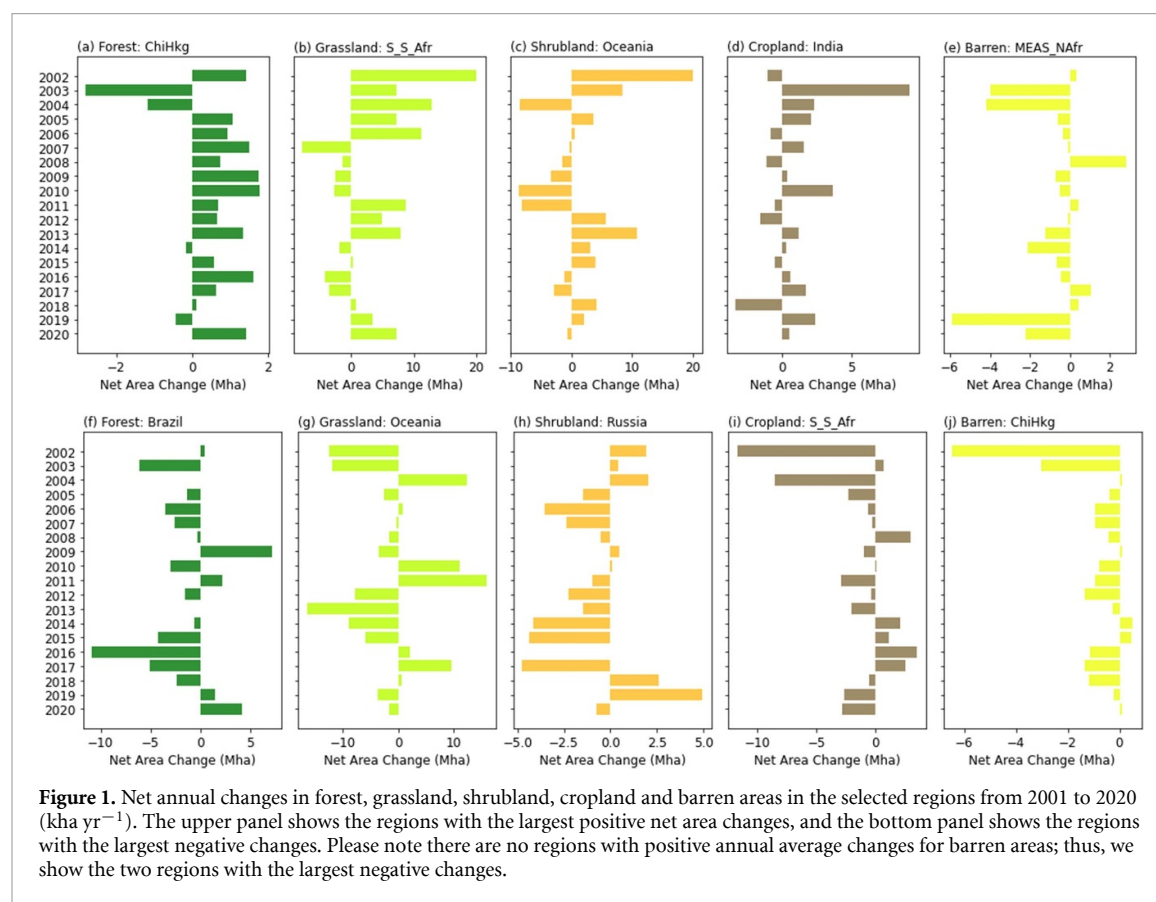
Category	Term	Definition	Example
No change	Stable	Stable refers to the pixels that represent no change in their land cover type between 2001 and 2020.	
Long term change	Gain	Gain refers to the pixels that were not classified as L_i in 2001 and then changed to L_i and remained in the new land cover type for the rest of the years (≥ 5 years).	
Long term change	Loss	Loss refers to the pixels that were classified as L_i in 2001 but changed to L_j ($i \neq j$) and never changed to the original or other land cover types in the rest of the years (≥ 5 years).	
Intermittent change	Unstable	Unstable refers to the pixels that represent other types of changes in their land cover type between 2001 and 2020.	

Oceania experienced major negative changes in 2002–2003 and 2012–2015 (figure 1(g)). In shrubland areas, Oceania experienced significant positive changes in 2002–2003 (figure 1(c)). Russia

experienced negative changes in most years, especially in 2014–2017 (figure 1(h)). In cropland areas, India had the largest increase in 2003, and then the cropland area fluctuated between positive and

Table 4. Average net area changes by GTAP-BIO 19 regions from 2001 to 2020 (kha yr⁻¹).

Region	Forest	Grassland	Shrubland	Cropland	Barren	Water	Ice	Urban
USA	−105	717	−221	163	−439	−13	−125	24
EU27	22	44	−36	−46	−71	47	33	8
Brazil	−1373	895	−181	651	−5	10	0	2
Canada	248	12	−598	491	−4	−6	−146	3
Japan	−30	32	1	−4	0	0	0	2
ChiHkg	619	212	−218	186	−954	25	9	121
India	244	−932	−196	882	−41	18	18	8
C_C_Amer	226	318	−135	−186	−236	7	0	5
S_O_Amer	−1008	671	217	264	−124	−15	−8	3
E_Asia	63	408	−7	−25	−438	−3	0	2
R_SE_Asia	−176	114	−9	63	−2	1	−1	10
Mala_Indo	93	52	−2	−154	−1	2	0	11
R_S_Asia	97	156	257	112	−659	3	34	2
Russia	513	365	−751	−21	−72	−6	−33	4
Oth_CEE_CIS	59	904	−53	−52	−913	12	39	4
Oth_Europe	−116	85	34	2	−2	3	−5	0
MEAS_NAfr	46	124	573	192	−940	0	0	5
S_S_Afr	−1073	3652	−1062	−1192	−341	−6	0	22
Oceania	−152	−1299	1434	82	−39	−27	−2	3
Total	−1804	6529	−952	1407	−5281	51	−188	237



negative in the following years (figure 1(d)). Sub-Saharan Africa had the largest negative changes in 2002 and 2004 (figure 1(i)). In barren land, no major positive changes have been observed. Middle Eastern and North Africa and China had negative changes in most years (figure 1 panels (e) and (j)).

3.2. Long-term and intermittent changes

According to the definitions provided in table 3, among eight land covers, an average of 69% of the gains and 75% of the losses lasted more than 15 years (table S5). Of the global forest area, 75% was labeled as Stable from 2001 to 2020, 4% was marked as Gain, 5% was identified as Loss, and

Table 5. Percentage of Stable, Gain, Loss, and Unstable land cover changes from 2001 to 2020^a.

Type	Forest	Grassland	Shrubland	Cropland	Barren	Water	Ice	Urban
Stable	75%	47%	46%	56%	73%	88%	97%	95%
Gain	4%	10%	9%	9%	3%	2%	0%	4%
Loss	5%	9%	11%	9%	7%	2%	0%	0%
Unstable	16%	33%	33%	26%	17%	8%	3%	1%

^a Note that regional changes in forest, grassland, and cropland classified in Stable, Gain, Loss and Unstable groups are provided in table S7.

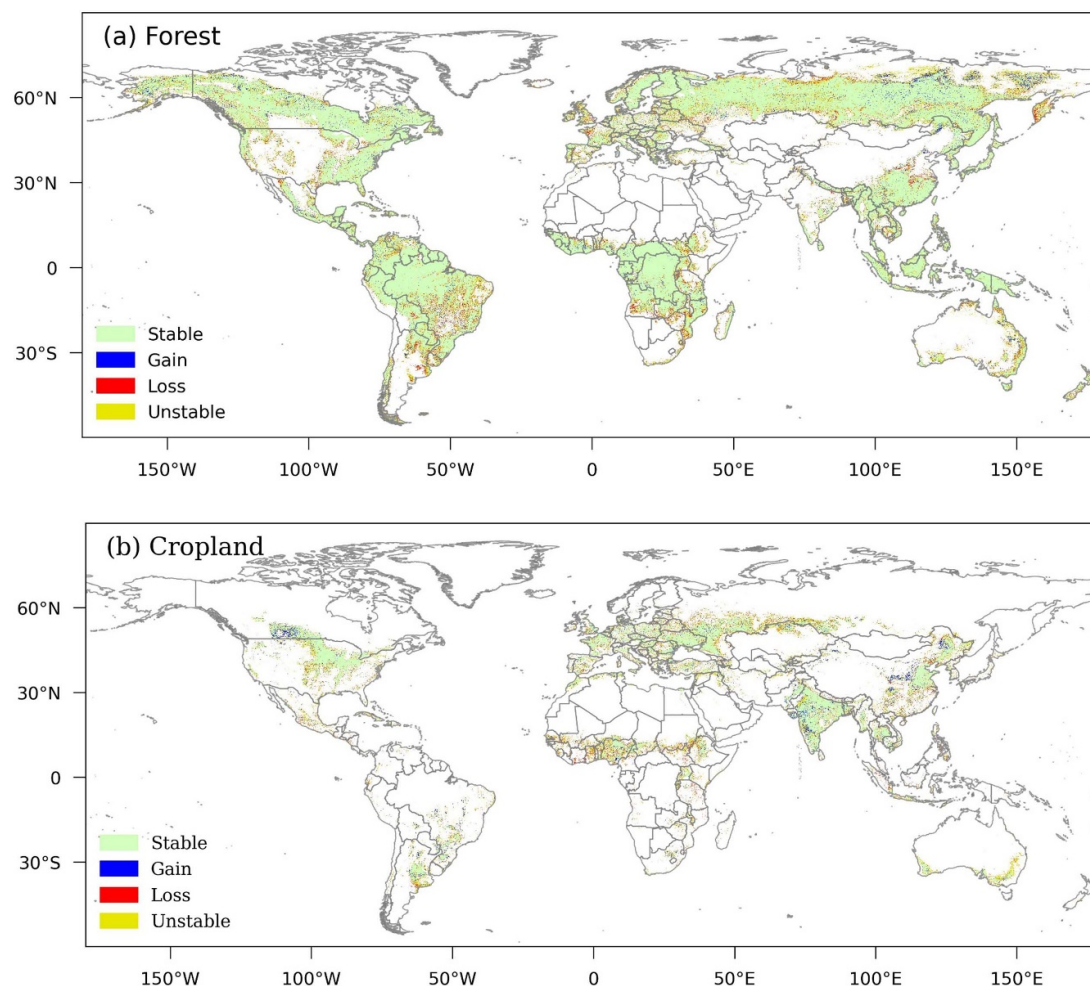


Figure 2. Land cover change of (a) forest and (b) cropland from 2001 to 2020. Note: High-resolution images are available in Chen *et al* (2024).

16% was recognized as Unstable (table 5). Brazil, the Rest of South America, and Sub-Saharan Africa were the hotspots of deforestation, marked as Loss (figure 2(a)). Deforestation in the Brazilian Amazon cut through the rainforest and formed a ‘herringbone’ pattern (figure S1(a)). Small clearing activities were also observed in the drier Cerrado regions (figure S1(b)). In sub-Saharan Africa, forest losses were widespread along the frontier of Miombo woodlands clearings (figure S1(d)). In Russia, the forest areas have experienced significant disturbances (marked as Loss) in regions such as the Yamalo-Nenets Autonomous Okrug and Kamchatka Peninsula (figure S1(e)).

Of the global cropland area, 56% was marked as Stable from 2001 to 2020, 9% was identified as Gain, 9% was labeled as Loss, and 26% was recognized as Unstable (table 5). Hence, a big portion of the global cropland area (26%) has temporarily moved to other land types and returned to crop production between 2001 and 2020. The global cropland expansion (Gain) hotspots were in Canada, Brazil, India, and China (figure 2(b)). Large cropland expansion was the dominant pattern in the Canadian Prairies and the west of peninsular India (figure S2 panels (a) and (c)). The cropland expansion area (Gain) was large in Brazil, but it consisted of small and concentrated patches across the continent (figure S2(b)). In

China, highly concentrated cropland expansion hotspots were observed in the northeastern and northern parts, known as China's 'corn belt' (figures S2 panels (d) and (e)). However, locations with the highest abandonment also had high levels of expansion (figure S2 panels (d) and (e)).

As for the other vegetation land cover, of the global grassland area, 47% was marked as Stable, 10% was identified as Gain, 9% was labeled as Loss, and 33% was recognized as Unstable (table 5). Grassland losses were widely distributed around the world but relatively concentrated in the Canadian Prairies, Southern Africa, Northeastern China, and Northern Australia (figure S5). However, grassland gains were concentrated in Eastern Africa, Kazakhstan, and Northern China (figure S5). The hotspots of unstable grassland were in Sub-Saharan Africa and Oceania (figure S5). Of the global shrubland area, 46% was marked as Stable, 9% was identified as Gain, 11% was labeled as Loss, and 33% was recognized as Unstable (table 5). The hotspots of shrubland gains were in Australia and Southern Africa, and those of shrubland losses were in Mexico, eastern Africa, northern China, and northern Russia (figure S6). The hotspots of unstable shrubland were in northern Russia and Oceania (figure S6).

For the non-vegetation land cover, 73% of the global barren area was labeled as Stable, 3% was identified as Gain, 7% was recognized as Loss, and 17% was marked as Unstable (table 5). Syria and Iraq have experienced large barren land gain, while many other regions, such as the USA, Kazakhstan, and China, have experienced barren land loss (figure S7). Of the global inland water bodies, 88%, 2%, 2%, and 8% were labeled as Stable, Gain, Loss, and Unstable, respectively (table 5). The losses and gains in inland water bodies were scattered globally, especially in northern America and Eastern Asia (figure S8). Two relatively large patches could be found in Great Salt Lake in the USA and Mackey Lake in Australia (figure S8). Of the global permanent snow and glaciers (Ice), 97% and 3% were labeled as Stable and Unstable with no major Gain or Loss (table 5). The unstable snow and glaciers were mainly in northern Canada and eastern Russia (figure S9). Of global urban land cover areas, 95%, 4%, 0%, and 1% were labeled as Stable, Gain, Loss, and Unstable, respectively (table 5). The hotspots of urban area gain appeared in eastern China (figure S10).

3.3. Identifying sources and fates of land cover change

In general, global forest losses were mainly changed to grassland, cropland, and shrubland from 2001 to 2020 (figure 3). However, in India, China, and the Rest of South Asia, most of the forest losses were changed to croplands (figure 3 panels (f), (g), and (m)). In Canada and Russia, forest areas were mainly

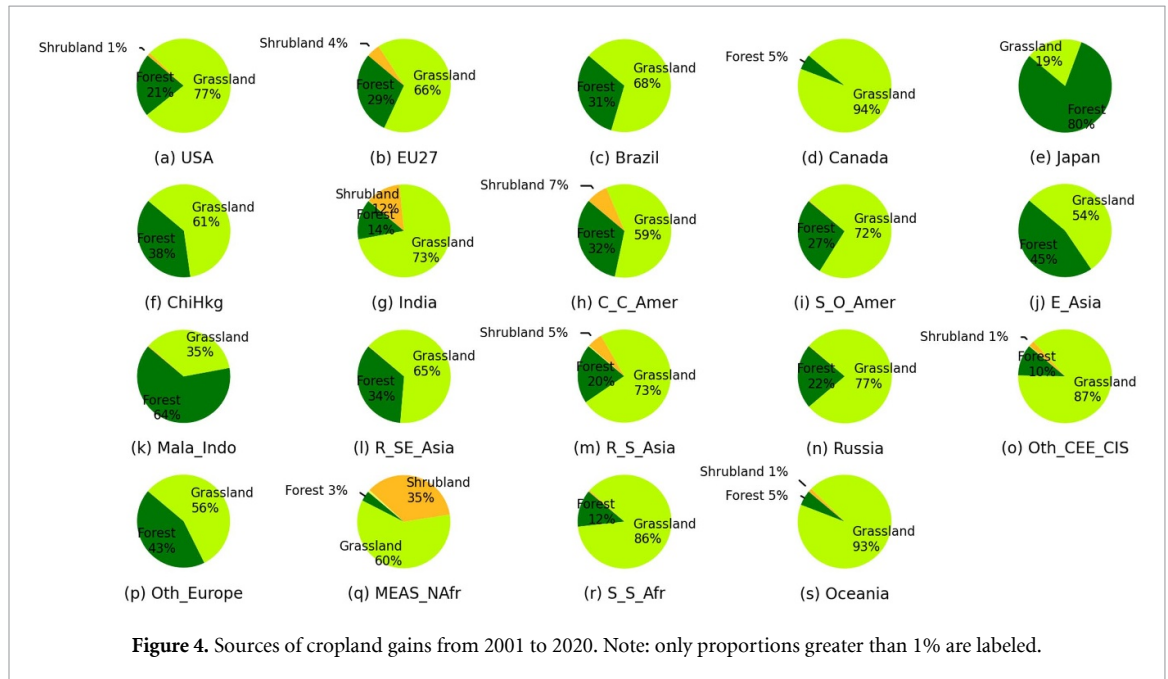
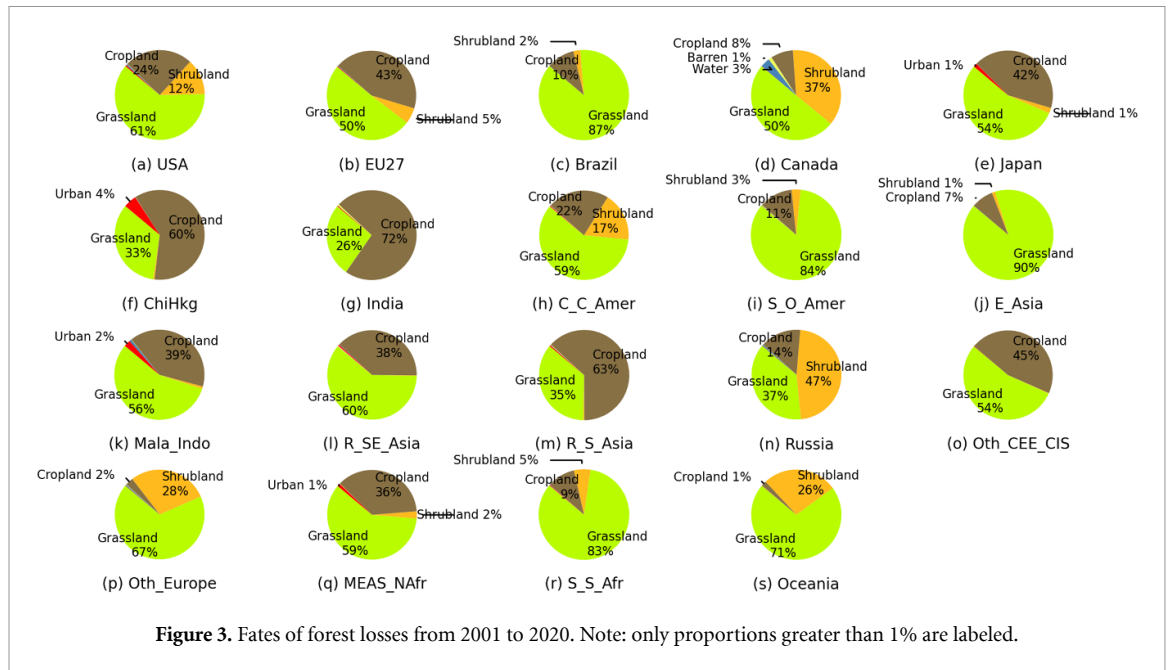
changed to grassland and shrubland (figure 3 panels (d) and (n)). In China, about 4% of forest losses were shifted to urban areas (figure 3(f)). This pattern was also observed in Japan (figure 3(e)), Malaysia and Indonesia (figure 3(k)), and Middle Eastern and North Africa (figure 3(q)).

Grasslands were the dominant sources for global cropland gains from 2001 to 2020 (figure 4). For example, over 90% of cropland gains came from grassland in Canada and Oceania. Forests were the second dominant source of global cropland gains, especially in Japan (figure 4(e)) and Malaysia and Indonesia (figure 4(k)). Besides grassland and forest, shrubland also contributed to the cropland gains in a few regions, e.g. Middle Eastern and North Africa (35%), India (12%), Central and Caribbean Americas (7%), EU27 (4%), and Rest of South Asia (5%).

4. Discussion

This study offered a novel perspective on land cover change by differentiating intermittent and long-term changes, which set it apart from the focus of current literature. Firstly, the results showed that grassland and shrubland each experienced 33% unstable changes, potentially due to various disturbances such as wildfires, drought, agricultural activities, insect infestations, and disease (Antwi *et al* 2008, Fu *et al* 2012). Secondly, most forest lands remained stable, with losses generally offset by gains. What was traditionally attributed to deforestation might primarily involve the unstable frontier that cycles between forest and other land classifications. For example, commercial forests cycle between cutting and replanting (Curtis *et al* 2018). Thirdly, cropland expansions previously identified in Sub-Saharan Africa and South America were found to be unstable in this research. This suggested that these areas might experience lower-frequency use for crop production rather than long-term gains in cropland. We emphasized that future land change analysis should differentiate intermittent and long-term changes in land cover to ensure a more accurate understanding of the dynamics involved.

Understanding the drivers of land cover change requires in-depth and on-the-ground research into local factors such as government policies, infrastructure investments, institutional capacities, and other factors that affect land cover changes (Efroymson *et al* 2016). We found that losses in forest areas were mainly converted to grassland, while gains in cropland areas were sourced from grassland losses (figures 3 and 4). This pattern may confirm that expansion in grassland and their return to cropland are the common low-risk land management practices after land clearing. Various reasons such as land grabbing incentives, additional demand for wood and wood products, mining activities, construction and



development plans, additional demand for meat and other livestock products, more demand for crops, and lack of effective public forces to control deforestation may jointly contribute to deforestation (Laurance *et al* 2009, Barber *et al* 2014, Sedano *et al* 2016, Sonter *et al* 2017, Taheripour *et al* 2019, Engert *et al* 2024). While additional demands for crops could induce more demand for cropland, and that could directly cause deforestation, lack of investments in yield-improving technologies across the world, improper regulations that weaken adopting new seed technologies, and lack of biotechnology and good agricultural management to enhance crop yields in many countries could be drivers of deforestation around

the globe. Thus, we highlighted the need for more detailed analyses to better understand the drivers of land cover change.

It is important to acknowledge the uncertainties in land cover changes associated with MODIS data. In general, the classification error of the MCD12Q1 land cover product introduces uncertainty. According to Sulla-Menashe *et al* (2019), the overall accuracies of the LCCS2 layer, using a random sampling assessment, were estimated to be around 80% across all years and about 78% for 2001, the selected base year in this study. In addition, the use of a single year as the initial reference year, as performed in this study, may introduce uncertainty. Factors such as the occurrence

of extreme weather events and temporary fallowing or inactive production in the initial reference period may also influence analysis results (Singh *et al* 2017).

We conducted two sensitivity tests to partially address uncertainties associated with our analyses. The first test uses 2003 instead of 2001 as the reference year. Table S6 shows the results of this change regarding the cover changes classified as Stable, Gain, Loss, and Unstable. The results presented in this table showed some differences compared with the results associated with the time period of 2001–2020 presented in table 5. In general, the differences varied between 0% and 3%, except for the cases of unstable grassland ($40\% - 33\% = 7\%$), shrubland ($40\% - 33\% = 7\%$), and cropland ($32\% - 26\% = 6\%$), which were more than 3% and reached up to 7%. When we changed the base year from 2001 to 2003, we indeed shrunk the time horizon of the analysis from 20 years to 18 years, which altered the results to some extent. The second test evaluated changes in land cover classes for the ESA-CCI data set. The results are presented in table S4. Comparing the results presented in this table with those presented in table 4 obtained from MODIS data revealed major differences. For example, figure S4 shows changes in Brazilian forest areas over time obtained from MCD12Q1 and ESA-CCI gridded data sets. Both data sets confirmed deforestation in Brazil, but with different magnitudes and trajectories (figure S1). The differences could be due to different sensor designs, classification methods, and training data reading (Wang *et al* 2023). This comparison confirmed that different satellite data sets provided different land cover changes, indicating that satellite land cover data products should be carefully assessed and critically reviewed to ensure that they represent accurate information.

The accuracy of assessing land cover changes is a fundamental need. Land cover changes could consequently influence surface temperature (Luyssaert *et al* 2014), biodiversity, air quality (Vadrevu *et al* 2017), and biogeochemical cycles (Le Quéré *et al* 2013, Arneth *et al* 2014). For instance, converting grassland to cropland may reduce SOC and lead to greenhouse gas emissions (Alidoust *et al* 2018). On the other hand, the effects of such transitions on SOC are highly context-dependent and influenced by prior land conditions and land management practices after land cover changes. Poorly managed grasslands often experience declining SOC, and the transition of pasture land to croplands, when accompanied by sustainable practices, can facilitate SOC recovery. For example, Wang *et al* (2008) demonstrated that properly managed croplands could restore SOC levels in degraded grasslands. This underscored the need for accurate assessment of land cover changes. Major efforts should be made to evaluate and improve the

accuracy of the available sources of data that represent changes in land cover over time.

5. Conclusion

Understanding how global land cover has changed across time and space is essential to identify more effective policies and land management practices to mitigate detrimental land cover changes across the world. This study differentiated long-term and intermittent land cover changes at the global scale using a well-known gridded data set, MCD12Q1. We found that global barren lands, forests, shrublands, and snow-covered areas decreased while grasslands, croplands, urban areas, and water bodies increased from 2001 to 2020. However, relatively large portions of the observed changes in forest, grassland, shrubland, and cropland were intermittent changes. Brazil, the Rest of South America and Sub-Saharan Africa were the hotspots of deforestation, most of which were changed to grasslands. The global cropland expansion hotspots were Brazil, Canada, China, India, and the Rest of South America, which were mainly converted from grassland. On the other hand, a large amount of shrublands were changed to forest in temperate regions. Barren areas in the USA, Kazakhstan, and China were converted to grasslands. The paper addressed uncertainties in assessing land cover changes using satellite data.

Data availability statement

All data that support the findings of this study are included within the article (and any supplementary files).




Acknowledgement

The authors would like to thank the anonymous reviewers of this article for their helpful comments and constructive suggestions. This research was partially funded by the US Federal Aviation Administration Office of Environment and Energy through ASCENT, the FAA Center of Excellence for Alternative Jet Fuels and the Environment, project 001 through FAA Award Number 13-C-AJFEPU under the supervision of P. Lobo. Any opinions, findings, conclusions, or recommendations expressed in this publication are those of the authors and do not necessarily reflect the views of the FAA. The research was also supported by NASA projects 80NSSC22K1252 and 80NSSC21K1710.

ORCID iDs

Shuo Chen  <https://orcid.org/0009-0001-8125-0903>

Qianlai Zhuang  <https://orcid.org/0000-0002-4536-9851>

Farzad Taheripour  <https://orcid.org/0000-0002-2652-3403>
 Ye Yuan  <https://orcid.org/0000-0003-1330-4049>
 Lauren Benavidez  <https://orcid.org/0009-0009-9348-8394>

References

- Alidoust E, Afyuni M, Hajabbasi M A and Mosaddeghi M R 2018 Soil carbon sequestration potential as affected by soil physical and climatic factors under different land uses in a semiarid region *CATENA* **171** 62–71
- Antwi E K, Krawczynski R and Wiegand G 2008 Detecting the effect of disturbance on habitat diversity and land cover change in a post-mining area using GIS *Landscape Urban Plan.* **87** 22–32
- Arneth A, Brown C and Rounsevell M D A 2014 Global models of human decision-making for land-based mitigation and adaptation assessment *Nat. Clim. Change* **4** 550–7
- Barber C P, Cochran M A, Souza C M and Laurance W F 2014 Roads, deforestation, and the mitigating effect of protected areas in the Amazon *Biol. Conserv.* **177** 203–9
- Bryan B A et al 2018 China's response to a national land-system sustainability emergency *Nature* **559** 193–204
- Busch J, Amarjargal O, Taheripour F, Austin K G, Siregar R N, Koenig K and Hertel T W 2022 Effects of demand-side restrictions on high-deforestation palm oil in Europe on deforestation and emissions in Indonesia *Environ. Res. Lett.* **17** 014035
- Chen S, Zhuang Q and Taheripour F 2024 Global land cover change maps from 2001 to 2020 *Zenodo* (<https://doi.org/10.5281/zenodo.14237104>)
- Copenhaver K L 2022 Combining tabular and satellite-based datasets to better understand cropland change *Land* **11** 714
- Copenhaver K and Mueller S 2024 Considering historical land use when estimating soil carbon stock changes of transitional croplands *Sustainability* **16** 734
- Curtis P G, Slay C M, Harris N L, Tyukavina A and Hansen M C 2018 Classifying drivers of global forest loss *Science* **361** 1108–11
- Defourny P et al 2017 Land cover climate change initiative—product user guide v2. Issue 2.0 (available at: http://maps.elie.ucl.ac.be/CCI/viewer/download/ESACCI-LC-Ph2-PUGv2_2.0.pdf)
- Efroymson R A, Dale V H, Kline K L, McBride A C, Bielicki J M, Smith R L, Parish E S, Schweizer P E and Shaw D M 2013 Environmental indicators of biofuel sustainability: what about context? *Environ. Manage.* **51** 291–306
- Efroymson R A, Kline K L, Angelsen A, Verburg P H, Dale V H, Langevelde J W A and McBride A 2016 A causal analysis framework for land-use change and the potential role of bioenergy policy *Land Use Policy* **59** 516–27
- Engert J E, Campbell M J, Cinner J E, Ishida Y, Sloan S, Supriatna J, Alamgir M, Cislowski J and Laurance W F 2024 Ghost roads and the destruction of Asia-Pacific tropical forests *Nature* **629** 370–5
- Fao F 2024 FAOSTAT domain land cover *Methodological Note* (available at: www.fao.org/faostat/en/#data/LC)
- Friedl M and Sulla-Menashe D 2022 MODIS/Terra+Aqua land cover type yearly L3 Global 500m SIN Grid V061 (available at: <https://lpdaac.usgs.gov/products/mcd12q1v061/>)
- Fu L, Bo T, Du G and Zheng X 2012 Modeling the responses of grassland vegetation coverage to grazing disturbance in an alpine meadow *Ecol. Modelling* **247** 221–32
- Goldewijk K K, Beusen A, Doelman J and Stehfest E 2017 Anthropogenic land use estimates for the Holocene—HYDE 3.2 *Earth Syst. Sci. Data* **9** 927–53
- Jing Q et al 2024 Analysis of the spatiotemporal changes in global land cover from 2001 to 2020 *Sci. Total Environ.* **908** 168354
- Laurance W F, Goosem M and Laurance S G W 2009 Impacts of roads and linear clearings on tropical forests *Trends Ecol. Evol.* **24** 659–69
- Le Quéré C, Andres R J, Boden T, Conway T, Houghton R A, House J I, Marland G, Peters G P, van der Werf G R and Ahlström A 2013 The global carbon budget 1959–2011 *Earth Syst. Sci. Data* **5** 165–85
- Liu F, Zhang Z, Zhao X, Wang X, Zuo L, Wen Q, Yi L, Xu J, Hu S and Liu B 2019 Chinese cropland losses due to urban expansion in the past four decades *Sci. Total Environ.* **650** 847–57
- Liu H, Gong P, Wang J, Clinton N, Bai Y and Liang S 2020 Annual dynamics of global land cover and its long-term changes from 1982 to 2015 *Earth Syst. Sci. Data* **12** 1217–43
- Liu X, Yu L, Li W, Peng D, Zhong L, Li L, Xin Q, Lu H, Yu C and Gong P 2018 Comparison of country-level cropland areas between ESA-CCI land cover maps and FAOSTAT data *Int. J. Remote Sens.* **39** 6631–45
- Luyssaert S et al 2014 Land management and land-cover change have impacts of similar magnitude on surface temperature *Nat. Clim. Change* **4** 389–93
- Piao S et al 2020 Characteristics, drivers and feedbacks of global greening *Nat. Rev. Earth Environ.* **1** 14–27
- Qiu B, Li H, Tang Z, Chen C and Berry J 2020 How cropland losses shaped by unbalanced urbanization process? *Land Use Policy* **96** 104715
- Sedano F, Silva J A, Machoco R, Meque C H, Siteo A, Ribeiro N, Anderson K, Ombe Z A, Baule S H and Tucker C J 2016 The impact of charcoal production on forest degradation: a case study in Tete, Mozambique *Environ. Res. Lett.* **11** 094020
- Shukla P R, Skeg J, E C Buendia, Masson-Delmotte V, Pörtner H-O, Roberts D, Zhai P, Slade R, Connors S and Van Diemen S 2019 Climate Change and Land: an IPCC special report on climate change, desertification, land degradation, sustainable land management, food security, and greenhouse gas fluxes in terrestrial ecosystems (available at: <https://www.ipcc.ch/srccl/>)
- Singh N, Kline K L, Efroymson R A, Bhaduri B and O'Banion B 2017 Uncertainty in estimates of bioenergy-induced land use change *Bioenergy and Land Use Change* (American Geophysical Union (AGU)) pp 141–53
- Song X-P, Hansen M C, Stehman S V, Potapov P V, Tyukavina A, Vermote E F and Townshend J R 2018 Global land change from 1982 to 2016 *Nature* **560** 639–43
- Sonter L J, Herrera D, Barrett D J, Galford G L, Moran C J and Soares-Filho B S 2017 Mining drives extensive deforestation in the Brazilian Amazon *Nat. Commun.* **8** 1013
- Sulla-Menashe D, Gray J M, Abercrombie S P and Friedl M A 2019 Hierarchical mapping of annual global land cover 2001 to present: the MODIS collection 6 land cover product *Remote Sens. Environ.* **222** 183–94
- Taheripour F, Hertel T W and Ramankutty N 2019 Market-mediated responses confound policies to limit deforestation from oil palm expansion in Malaysia and Indonesia *Proc. Natl Acad. Sci.* **116** 19193–9
- Tyukavina A et al 2022 Global trends of forest loss due to fire from 2001 to 2019 *Front. Remote Sens.* **3** 825190
- Vadrevu K, Ohara T and Justice C 2017 Land cover, land use changes and air pollution in Asia: a synthesis *Environ. Res. Lett.* **12** 120201
- Wang Y, Sun Y, Cao X, Wang Y, Zhang W and Cheng X 2023 A review of regional and global scale Land Use/Land Cover (LULC) mapping products generated from satellite remote sensing *ISPRS J. Photogramm. Remote Sens.* **206** 311–34
- Wang Z-P, Han X-G and Li L-H 2008 Effects of grassland conversion to croplands on soil organic carbon in the temperate Inner Mongolia *J. Environ. Manage.* **86** 529–34
- Winkler K, Fuchs R, Rounsevell M and Herold M 2021 Global land use changes are four times greater than previously estimated *Nat. Commun.* **12** 2501
- Zhao X, Taheripour F, Malina R, Staples M D and Tyner W E 2021 Estimating induced land use change emissions for sustainable aviation biofuel pathways *Sci. Total Environ.* **779** 146238

Technical Report Documentation Page

1. Report No.	2. Government Accession No.	3. Recipient's Catalog No.	
4. Title and Subtitle		5. Report Date	
		6. Performing Organization Code	
7. Author(s)		8. Performing Organization Report No.	
9. Performing Organization Name and Address		10. Work Unit No. (TRAIS)	
		11. Contract or Grant No.	
12. Sponsoring Agency Name and Address		13. Type of Report and Period Covered	
		14. Sponsoring Agency Code	
15. Supplementary Notes			
16. Abstract			
17. Key Words		18. Distribution Statement	
19. Security Classif. (of this report) Unclassified	20. Security Classif. (of this page) Unclassified	21. No. of Pages	22. Price